JOURNAL OF MATERIALS SCIENCE 26 (1991) 274–284

# Structure and mechanical properties of corn kernels: a hybrid composite material

S. S. SINGH*, M. F. FINNER‡, P. K. ROHATGI*, F. H. BUELOW‡, M. SCHALLER*
* *University of Wisconsin–Milwaukee Materials Department, PO Box 784, Milwaukee, Wisconsin 53201, USA*
‡ *University of Wisconsin–Madison, 460 Henry Mall, Madison, Wisconsin 53706, USA*

The mechanical properties of corn kernels were evaluated at three levels of kernel structure, varying in the proportions of horny endosperm, and six levels of moisture content in the range of 6 to 34% (wet basis) under a compression mode of loading. The observed values of ultimate stress, modulus of elasticity, modulus of toughness and modulus of resilience varied from 8 to 82 MPa, 20 to 480 MPa, 0.8 to 4.4 MJ $m^{-3}$ and 0.2 to 0.8 MJ $m^{-3}$, respectively, within the experimental range. Each of these properties decreased in magnitude as the moisture content increased. The microscopic study revealed that the resistance of kernels to fracture was predominantly influenced by the kernel structure. The size of cracks increased with increasing strain or decreasing proportion of the horny endosperm in the kernels. The viscoelastic behaviour of the kernels was determined at two levels of kernel structure, five levels of kernel moisture (12 to 34%) with three deformation rates (1.27, 5.08 and 12.7 mm $min^{-1}$) by means of stress relaxation tests. The analysis of the test data suggested that the hybrid composite kernels were hydrorheologically simple materials.

## 1. Introduction

Biological materials are largely made up of polymeric substances and they contain significant amounts of water. These materials exhibit both elastic and viscous responses to external forces. Thus, the characterization of the mechanical responses of these materials requires the use of the theory of viscoelasticity. Compared with synthetically prepared engineering materials, the biomaterials derived from plant, animal or human bodies are quite complex and non-homogeneous in nature. The mechanical behaviour of solid biomaterials deviates substantially from that of a Hookean body, and the liquid in biological materials also deviates greatly from a Newtonian liquid. Further complications result from the natural shape, size and rigidity when applying principles of theoretical mechanics and testing techniques in the evaluation of the mechanical behaviour of biomaterials. In spite of all these limitations, researchers have shown that the mechanical behaviour of biological materials can be partially understood by the use of linear viscoelastic theory when applied stresses are sufficiently small [1–9].

In this investigation corn grain was selected as a test biomaterial because of current interest in developing high fracture resistance in this grain against the random impacts encountered in material-handling machines. Most of the previous studies on grain were concerned mainly with the determination of the mechanical responses for a particular strain of a grain [10–12]. The effects of the kernel macro- and microstructures on the mechanical responses of the grains have not been investigated in any detail. The major objective of this research was to determine the mechanical and viscoelastic behaviour of intact corn kernels (kernels in their natural shapes) as a function of the kernel structure and moisture content.

## 2. Previous studies

Time-dependent stress and strain behaviours have been extensively investigated for a number of biomaterials [1, 4, 7]. Several studies have also been directed towards developing relationships between the structure and the mechanical behaviour of biological materials [7, 8, 13–16]. However, very limited information is available on the mechanical responses of cereal grains as influenced by their kernel structures [11].

The mechanical properties of grains have been investigated by a number of researchers [4, 5, 10–12, 17]. A study showed that, when a wheat grain was subjected to uniaxial compression, it behaved as an elastic–plastic–viscous body exhibiting creep, stress relaxation and elastic after-effects [4]. The mechanical properties of corn kernels have been determined by using various loading devices including parallel plate [4, 10, 12, 17], cylindrical indentor [10, 17] and spherical indentor [10, 17]. In general the kernel strength properties decreased with increasing moisture content. The cut beam of corn horny endosperm has been employed to determine its fracture parameters [18]. It was reported that both the fracture toughness and the critical stress intensity factors were insensitive to moisture and temperature, but were


0022–2461/91 $03.00 + .12 

strongly influenced by the presence of a notch of any length.

The viscoelastic behaviour of corn in tension and in bending were determined through the use of cut samples of the horny endosperm [19, 20]. Cutting or shaping of a biological material may alter its structural mechanics and resultant mechanical behaviour, more so for small grains such as cereal grains [5]. Therefore, in order to obtain realistic data on the mechanical responses of cereal grains, as far as possible, intact grains should be tested.

Very limited information is, however, available on the viscoelastic behaviour of intact corn kernels, especially under the compression mode of loading. Since grains are more frequently subjected to compressive loads than to tensile or bending loads, the compressive mode of loading was adopted in this investigation.

## 3. Experimental details

An Instron testing machine (model 1130) was used to measure the kernel responses to compressive loadings by using parallel plates. A simple technique was adopted to determine the contact area (load-bearing area) of the individual kernels during the loading process. In this method, 30 mm × 30 mm pieces of both plain and carbon paper were taped on to the loading face of the top plate to record the carbon impression of the contact surface of the grain during loading. This impression represented the actual contact area during compression. The impressions were then traced on transparent films with black ink and their areas were measured with an area meter (LI-3100). The area under the load–deformation curve was measured by using a digital microcomputer system equipped with Talos digitizing tablet.

A tester was also designed, similar to the apparatus used in the candling technique, to measure stress cracks in the test kernels. Stress cracks are macrocracks generated due to drying stresses [21]. The tester consisted essentially of a metallic box in which a light source (60 W bulb), a reflector and a lens were arranged so as to direct bright light towards the central opening in the lid on which kernels were placed for stress crack examination.

Two types of corn species (dent and flint corn) were selected in this investigation. In dent corn horny endosperm is wrapped around the sides of the kernels but not at the very top; in the flint kernels the floury endosperm is completely encased by the horny endosperm. Three different types of kernel structures were obtained by selecting kernels of two dent corn hybrids $H_1$ ($GGC_{11}$) and $H_2$(BS 13 $(S_2)C_1$), and one flint corn $H_3$(Argentine). The $H_1$ has the lowest ratio of horny to floury endosperm, and $H_3$ had the highest ratio of horny to floury endosperm. The kernel densities for $H_1$, $H_2$ and $H_3$ were 1249, 1252 and 1346 kg m$^{-3}$, respectively, at a moisture content of 9% (wet basis). The samples were harvested manually at moisture contents ranging between 35 and 40 wt %. The various levels of kernel moisture content were obtained by drying the samples with forced air at 21 °C. The conditioned samples were kept in sealed plastic bottles and stored in a refrigerator.

A Hitachi S-570 scanning electron microscope was used to study the microstructure of the corn kernels. For the electron microscopy sections of the kernels were polished to expose the mid-longitudinal face. The polished specimens were sputter coated with 12 nm gold for microscopic examination.

All of the test kernels were checked for stress cracks using the stress crack tester, and the kernels chosen for testing were relatively free from stress cracks. Before loading, the thickness of each kernel was determined with a micrometer. The individual kernels with germ side down were cemented to the bottom plate using a quick-setting adhesive.

In mechanical properties tests, each kernel was loaded until rupture occurred, and the resultant load–deformation behaviour was recorded. A constant deformation velocity of 1.27 mm min$^{-1}$ was used in all of the tests. The kernel densities were determined by means of a liquid-displacement technique. Twenty kernels were tested for each experimental condition.

The viscoelastic behaviour of the intact kernels was determined by means of stress relaxation tests. In these tests a kernel was subjected to a constant strain of 0.045 and the resultant force as a function of time was recorded for a duration of 450 sec. Preliminary tests indicated that kernels developed cracks at deformation velocities in excess of 12.7 mm min$^{-1}$, especially at low kernel moisture contents. Therefore, a maximum deformation velocity of 12.7 mm min$^{-1}$ could be used for the viscoelastic tests. The tests were carried out at three deformation velocities (1.27, 5.08 and 12.70 mm min$^{-1}$), five levels of kernel moisture content ranging between 12 and 34%, and two levels of kernel structure ($H_2$ and $H_3$). Ten replications were conducted for each test condition.

## 4. Composition and structure of the test kernels

In order to interpret the mechanical behaviour of a grain, it is essential to understand its structure and chemical composition. A corn kernel is composed of four major parts: the pericarp (hull or bran), germ (embryo), endosperm and tip cap as shown in Fig. 1

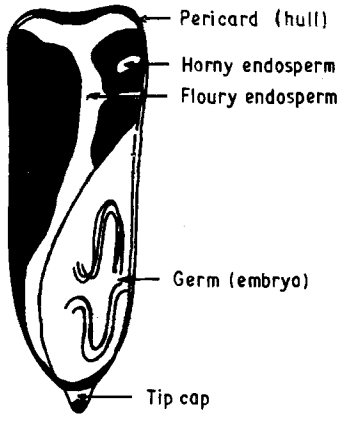


*Figure 1* Major structural element of a corn kernel.

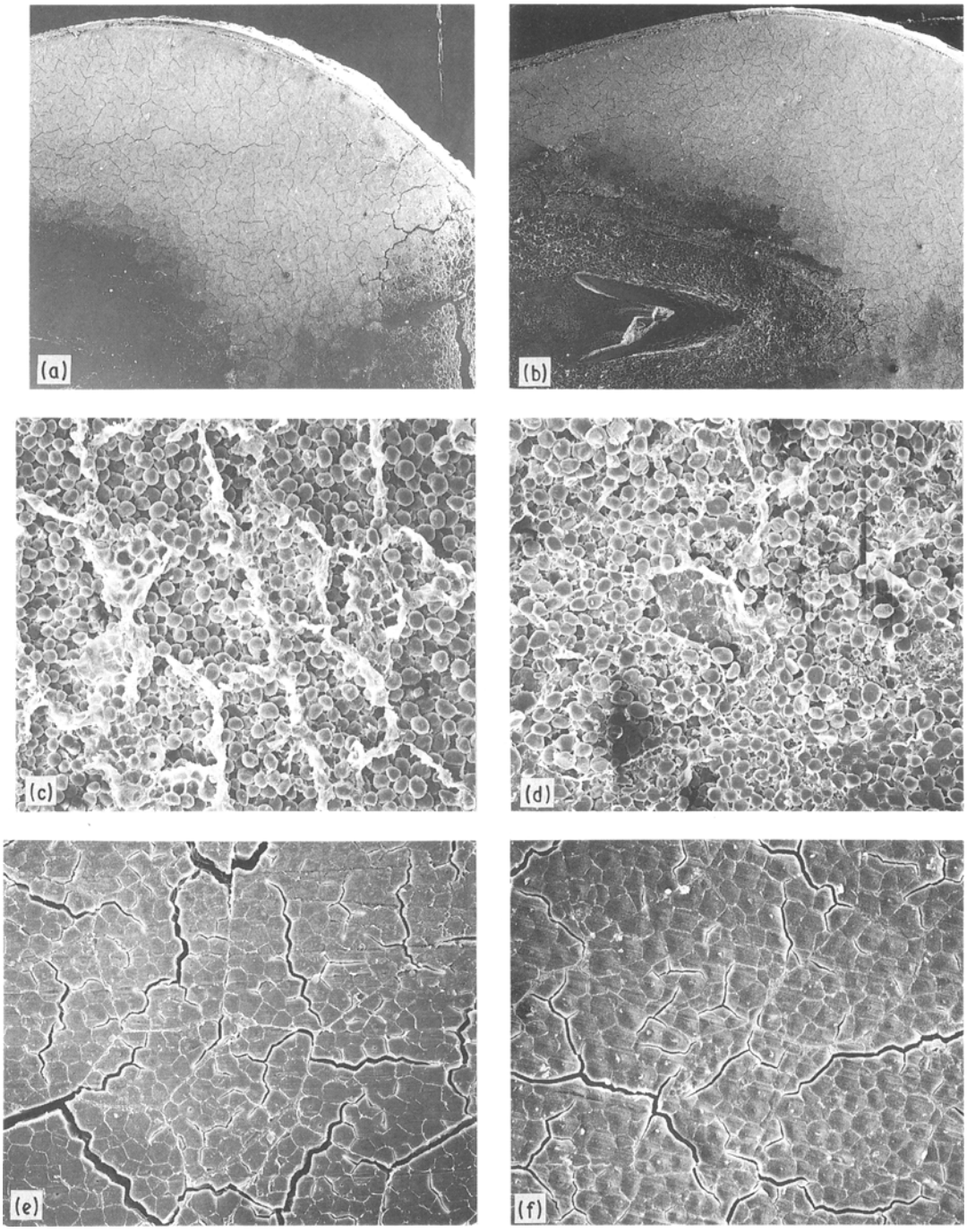


*Figure 2* Micrographs of the test kernels: (a) dent kernel ( × 12), (b) flint kernel ( × 12), (c) dent floury endosperm ( × 175), (d) flint floury endosperm ( × 175), (e) dent horny endosperm ( × 240) and (f) flint horny endosperm ( × 240).

[22, 23]. The approximate composition of the kernel is endosperm 82%, germ 12%, pericarp (hull) 5% and tip 1%. The major mechanical strength of this grain depends strongly on its endosperm structure. The corn endosperm is made up of two components: floury endosperm and horny endosperm. The ratio of horny to floury endosperm depends heavily on the genetic characteristics of the kernels.

Photomicrographs of the kernels are shown in Fig. 2. The typical shape of the floury endosperms cells are approximately polyhedral in shape and filled with spherical starch granules. The size of these cells and starch granules, although different from kernel to kernel and with location in the endosperm, were not influenced by the type of corn species tested. Cells of the floury endosperm ranged from 60 μm × 50 μm to 190 μm × 90 μm. Starch granules varied from 3 to 18 μm. Strings or irregular patches on the surface of the granules are remnants of the thin protein matrix. The horny endosperm cells are more sharply polyhedral and larger than the floury endosperm cells for both species. The cell size of the dent horny endosperm and the flint horny endosperm varied from 180 μm × 50 μm to 220 μm × 100 μm. The interior of these cells is tightly filled with starch grains embedded in a much heavier protein matrix than that observed

in the floury endosperm for both of the species. The average size of the starch grains in the horny endosperm of the dent and flint kernels was about 10 μm. The surfaces of the starch granules are angled because they are closely packed (Fig. 2). Profiles of the protein matrix were seen as irregular masses surrounding each starch grain. Also, surrounding the starch grains are smaller granules, approximately 0.5 to 2 μm, which probably represent part of the protein matrix.

It is known that starch is a polysaccharide in which the monomer unit is glucose. The starch granules in corn contain two kinds of molecules: amylose and amylopectin [24]. Amylose is essentially a linear molecule which has about 1000 glucose units. Amylopectin is a branched molecule which may contain 40 000 or more glucose units. The main fractions of corn protein are albumens, globulins, prolamines and glutelins [23]. The protein is made of a complex nitrogeneous organic compound of high molecular weight that contains α-amino acids as their basic structural units [25].

Previous studies have indicated that at various locations the molecules in the protein film in the corn endosperm are preferentially oriented [24]. Due to this unique structural arrangement in protein, powerful intermolecular binding forces, similar to those observed in oriented polymers, are expected, which probably gives the kernels their toughness. The ratio of starch to protein has been reported to be 11:1 in floury endosperm and 6:1 in the horny endosperm [24].

From the above description, it is clear that a corn endosperm is a polymer–polymer biocomposite material in which both the reinforcing filler or particle (starch) and matrix (protein) are made of natural polymeric substances. The kernel material is, therefore, a hybrid composite whose strength can vary from point to point because of the variations in the kernel structure. Thus, the mechanical properties of this grain would depend on the characteristics of the protein matrix and the starch granules, their volume percentages and their spatial distribution, and on the bond between the matrix and the starch granules.

## 5. Viscoelastic models of biomaterials

As described previously, the kernels have molecular structures similar to high polymers. Therefore, it is assumed that the effects of molecular structure on the mechanical behaviour of the kernels would follow the same general trend as that observed in the case of high polymers [4, 26]. The viscoelastic behaviours of biomaterials are most widely interpreted in terms of mechanical models. These models consist of some combinations of springs as the elastic elements and dashpots as the viscous elements. Various types of model have been used in representing the rheological behaviour of biomaterials [1, 2, 4, 6]. Two models, namely the Kelvin and Maxwell models, are most commonly used. A Kelvin model consist of a spring and a dashpot in parallel. Under a constant stress the Kelvin model exhibits creep behaviour [4]. The simplest Maxwell model, composed of a spring and a dashpot in series, is used to represent the stress relaxation behaviour of linear viscoelastic materials [26]. Due to the complex mechanical behaviour of most biomaterials, the single-element Maxwell model is often inadequate to describe the viscoelastic behaviour of the biomaterials. Therefore, a generalized Maxwell model consisting of several Maxwell elements with a spring in parallel is preferred (Fig. 3). Under the application of constant strain or deformation, the viscoelastic function exhibited by the model is of the form

$$E(t) = \sum_{i=1}^{n} E_i \exp(-t/T_i) + E_e \quad (1)$$

and

$$T_i = \eta_i / E_i \quad (2)$$

where $E(t)$ is the relaxation modulus at time $t$, $n$ is an integer constant, $E_i$ is the decay modulus of the $i$th Maxwell element, $T_i$ is the time of relaxation of the $i$th Maxwell element, $E_e$ is the equilibrium modulus or modulus after infinite time and $\eta_i$ is the viscosity of the $i$th viscous element.

The viscoelastic response of biomaterials depends strongly on the moisture content and temperature. When the influence of moisture on the response of a material can be compensated for by shifting along the time axis horizontally, then the materials are considered hydrorheologically simple. In a similar fashion, if the temperature effects of a material can be shifted along the time axis, then the material is said to be thermorheologically simple.

With a view to explaining the meaning of a shifting of the curves, a plot of the relaxation modulus against the logarithmic time is presented in Fig. 4. The relaxation modulus at a moisture content $M$ can be expressed as [27]

$$E_M(\log_{10} t) = E_{M0}[\log_{10} t + f(M)] = E_s \quad (3)$$

where $t$ is time, $E_M$ and $E_{M0}$ are the relaxation modulus function at a moisture content of $M$ and $M_0$, respectively, $E_s$ is the relaxation modulus at a selected time and $f(M)$ is the horizontal shift in the logarithmic scale to superimpose both of the curves.

Let

$$a_M(M) = 10^{f(M)} \quad (4)$$

Then

$$f(M) = \log_{10} a_M(M) \quad (5)$$

in which $a_M$ is defined as the moisture shift factor, and is a function of the moisture content.

Substituting Equation 5 into Equation 3 yields

$$E_M(\log_{10} t) = E_{M0}(\log_{10} t + \log_{10} a_M) \quad (6)$$

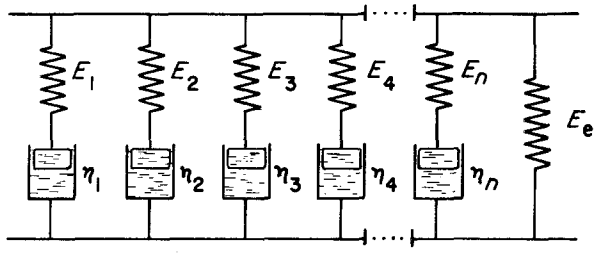


*Figure 3* Generalized Maxwell model.

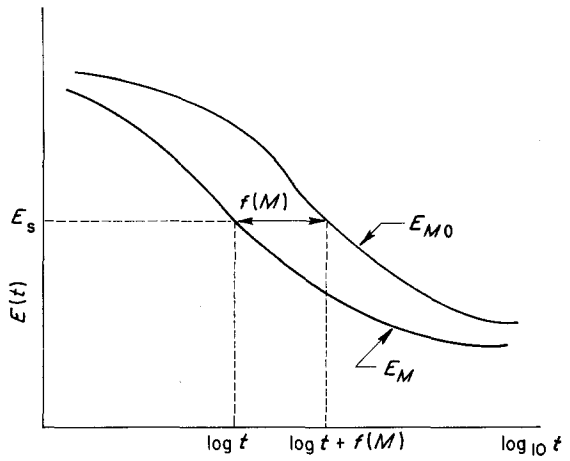


*Figure 4* A plot of $E(t)$ against $\log_{10} t$ for kernel moisture contents of $M$ and $M_0$.

or

$$E_M(\log_{10} t) = E_{M0}[\log_{10}(ta_M)] \quad (7)$$

Therefore,

$$E_M(t) = E_{M0}(ta_M) \quad (8)$$

Equation 8 reveals that $t$ units of time at moisture $M$ is equivalent to $(ta_M)$ units of time at moisture $M_0$. The shift function $a_M$ is inherent in the property of a viscoelastic material and should be determined experimentally. For $M < M_0$, $f(M) > 0$ and $a_M > 1$; for $M > M_0$, $f(M) < 0$ and $a_M < 1$; for $M = M_0$, $f(M) = 0$ and $a_M = 1$. A unit of time at moisture $M$ is equivalent to a $1/a_M$ units at moisture $M_0$.

Using the above procedure and the reasoning for time–temperature shifting of the relaxation curves, a temperature shift function $a_\theta$ can be determined. After determining the shift functions for both temperature and moisture content, the master relaxation modulus curve for the kernels may be represented by a generalized Maxwell model of the form

$$E(t, M, \theta) = \sum_{i=1}^{n} E_i \exp\left(-\frac{\alpha_i t}{a_\theta a_M}\right) + E_e \quad (9)$$

where $E(t, M, \theta)$ is the relaxation modulus as a function of time ($t$), moisture content ($M$) and temperature ($\theta$), $n$ is an integer constant, $a_\theta$ is the temperature shift factor, $a_M$ is the moisture shift factor, $\alpha_i$ is the inverse of the relaxation time ($T_i$) of the $i$th Maxwell element, $E_i$ is the decay modulus of the $i$th Maxwell element and $E_e$ is the equilibrium modulus.

Since in this investigation the temperature was kept constant, Equation 9 is reduced to

$$E(t, M) = \sum_{i=1}^{n} E_i \exp\left(-\frac{\alpha_i t}{a_M}\right) + E_e \quad (10)$$

## 6. Results and discussion

### 6.1. Mechanical properties

Theoretical models described in the Appendix can be used in determining the elastic properties of the corn endosperm. The models require the value of the input parameters such as shear modulus, volume fraction and Poisson's ratio of both the spherical particles (the starch granules) and the protein matrix. However, in the absence of readily available data on the shear modulus and Poisson's ratios of the participating constituents, and the crack extension being the primary mode of the deformation at the strain levels investigated, the theoretical prediction of the elastic properties has not been possible. Instead, experimental data were used to compare the properties of dent and flint corn kernels at relatively low strain levels.

The load–deformation behaviour of the kernel is shown in Fig. 5. In most cases the initial portion of the curve is approximately linear up to certain levels of deformation beyond which it became non-linear. The observed bioyield point represents the yield point in the biological materials. This is an indication of initial cell rupture in the cellular structure of the material [4]. The stress was expressed as force per unit area, and the strain was determined by dividing the kernel deformation by the initial kernel thickness. The modulus of resilience was determined by the area under the straight-line portion of the stress–strain curve. The modulus of toughness is represented by the area under the stress–strain curve up to the rupture point.

Analysis of the data showed that the ultimate stress, modulus of elasticity and modulus of toughness mostly increased as the proportions of the horny endosperm were increased from the level $H_1$ to $H_3$. However, the results were not significantly affected by the differences in the kernel structure of $H_1$ and $H_2$. The data obtained at various moisture levels were subjected to regression analysis. To account for differences resulting from the levels of kernel structures, the dummy variable concept was employed [28]. One dummy variable, $Z$, was found appropriate for the analysis as the responses of the two types of kernel ($H_1$ and $H_2$) could be described adequately by a single response curve. The results are presented for the moisture content range 6 to 34% (wet basis).

The mechanical behaviour of a kernel is strongly dependent on its moisture content. As water molecules enter the polymeric chain units, which are close to each other, the chains are forced to rearrange their relative positions, resulting in an increased volume of the kernel. In addition, the friction coefficient decreases with an increase in water content, as some of

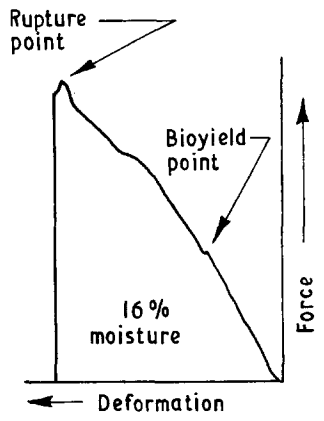


*Figure 5* A typical load–deformation curve for corn kernels.

the nearest neighbours of a polymer segment are solvent molecules and are highly mobile [10, 26]. Also, crack initiation and propagation will be affected by the levels of moisture present in the system. Consequently, the resistance to deformation decreases with an increase in water content of the kernel.

The stress–strain curves for the kernels $H_2$ and $H_3$ are shown in Figs 6 and 7, respectively. The test data showed that the ultimate stress, modulus of elasticity, modulus of toughness and modulus of resilience decreased exponentially as the moisture content increased. The ultimate stress values ranged between 8 and 82 MPa for the kernels tested. The regression model showed that the ultimate stress values for the flint kernel ($H_3$) were 1.23 times those obtained for the dent kernels (Fig. 8). The measured values of the modulus of elasticity for different types of material were in the range 20 to 480 MPa (Fig. 9). The regression model predicted substantially lower modulus values for the dent kernels; the dent kernel values were approximately 0.71 times those obtained for the flint kernels. The observed modulus of toughness values for the kernels varied between 0.8 and 4.4 MJ m$^{-3}$. The best-fit model for the modulus of toughness was

$$M_T = \exp(1.7 - 0.0576M + 0.106Z) \quad (r^2 = 93.7\%) \qquad (11)$$

where $M_T$ is the modulus of toughness (MJ m$^{-3}$), $M$ is the moisture content (% (wet basis)) and $Z$ is a dummy variable ($z = 0$ for dent kernel and $Z = 1$ for flint kernel).

The flint kernels showed a considerably higher modulus of roughness than the dent kernels. The modulus of resilience values were in the range 0.20 to 0.75 MJ m$^{-3}$. The modulus of resilience was relatively

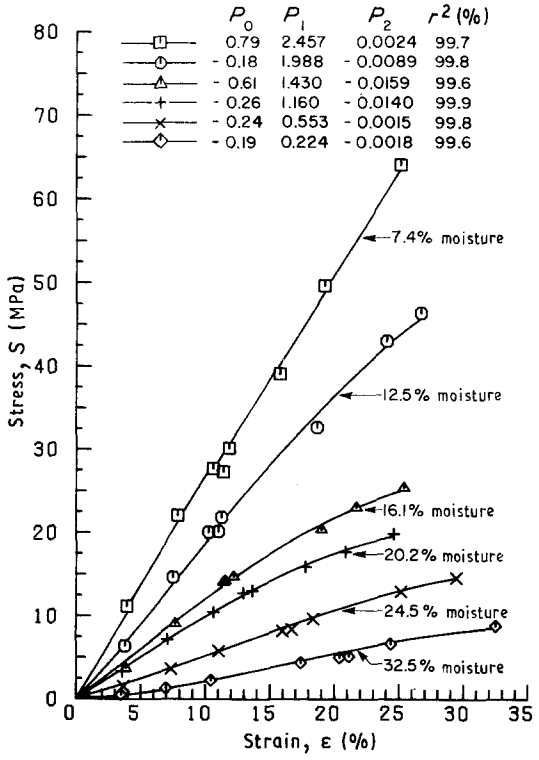


*Figure 6* Stress–strain relationship of the dent kernels ($H_2$) at six levels of moisture content. Model $S = P_0 + P_1\varepsilon + P_2\varepsilon^2$.

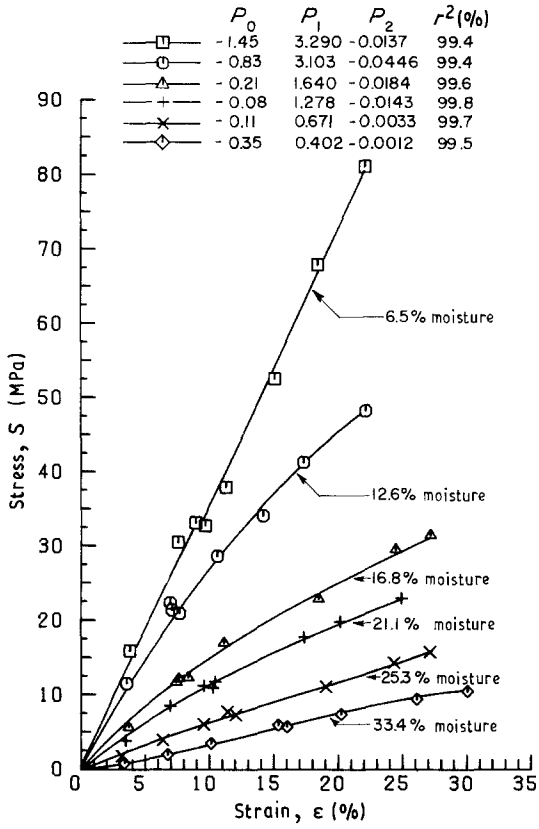


*Figure 7* Stress–strain relationship of the flint kernels ($H_3$) at six levels of moisture content. Model $S = P_0 + P_1\varepsilon + P_2\varepsilon^2$.

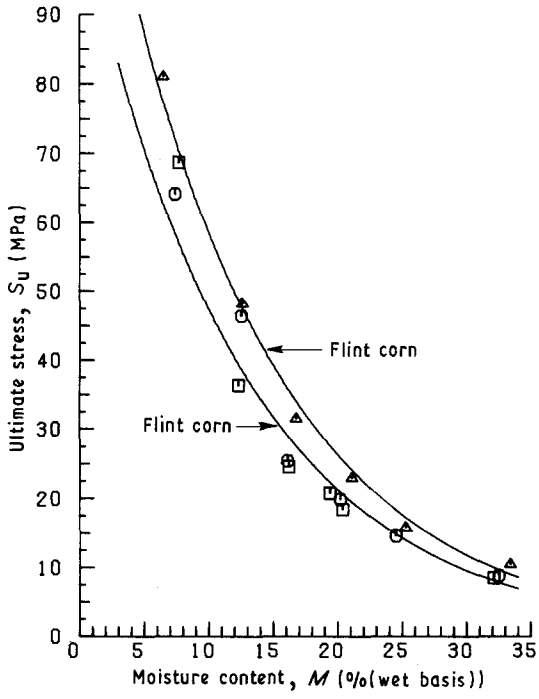


*Figure 8* Ultimate stress of the kernels as a function of moisture content. Regression model $S_u = \exp(4.659 - 0.080\ (M + 0.211Z)$, $r = 97.4\%$, $Z = 0$ for dent corn, $Z = 1$ for flint corn. (□) $H_{11}$ (GG $C_1$), (○) $H_{12}$ (BS 13 ($S_2$) $C_1$) and (△) $H_{13}$ Argentine flint.

unaffected by the kernel structures tested. The regression model for the modulus of resilience, based on the pooled data, was

$$M_R = 0.652 \exp(-0.0365M) \quad (r^2 = 65.6\%) \qquad (12)$$

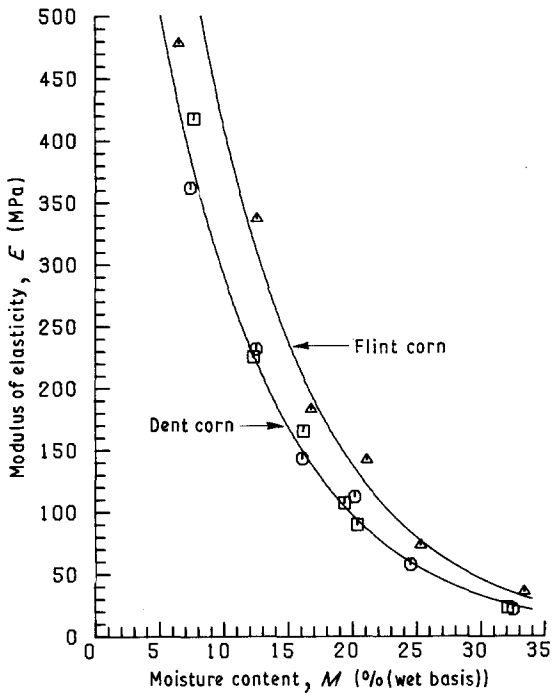


*Figure 9* Modulus of elasticity of the kernels as a function of moisture content. Regression model $E = \exp(6.772 - 0.1096M + 0.345Z)$, $r^2 = 98.7\%$, $Z = 0$ for dent corn, $Z = 1$ for flint corn. Key as Fig. 8.

where $M_R$ is the modulus of resilience (MJ m$^{-3}$) and $M$ is the moisture content (% (wet basis)).

## 6.2. Microscopic studies

Micrographs of the corn kernels subjected to the strains are shown in Figs 10 and 11. From the analysis of these micrographs, it was found that microcracks propagated (a) along the cell walls (intercellular), (b) through the cells (transcellular) and (c) intergranularly (at the interface of the starch granules and the protein matrix) due to the coalescence of voids in the protein matrix of the endosperms. At some places in the endosperms the cracks also propagated through the starch granules (transgranularly). Some of the starch granules of the floury endosperms were peeled off during deformation, which was apparently possible due to weak bonds between the granules and the protein matrix [24]. When various levels of compressive strain were applied, no significant alteration of individual cells or tissue pattern was observed. This may be attributed to the fact that when the kernels are loaded in the $Y$-direction they experience tensile strains in both the $X$-direction (longitudinally) and the $Z$-direction (transversely) (Fig. 12). These strains cause extensive cracks, and most of the strain energy of the kernels goes into the formation and extension of cracks instead of deforming the cells. Consequently, little distortion in either cells or starch granules was observed within the tested range. Most of the kernels as received were found to have microcracks due to the drying stresses. The size and number of cracks increased with the strain. The resultant network of cracks consisted of primary, secondary and tertiary cracks. In this investigation, primary cracks were selected to compare the fracture behaviour of the kernels due to the compressive loadings. Besides, no significant change in the direction of propagation of the major cracks was observed, particularly at low strain levels. This is understood to be due to the lower fracture resistance of the soft endosperm (floury endosperm regions). When the strain was increased from 15 to 25%, the maximum longitudinal crack length increased from 5.29 to 6.29 mm for dent and from 5.44 to 6.12 mm for flint kernels, whereas the increase in the transverse cracks ranged from 4.08 to 4.93 mm for dent and from 3.74 to 3.91 mm for flint (Table I). The maximum width of the longitudinal cracks increased from 102 to 493 μm and from 102 to 374 μm for dent and flint kernels, respectively. Under the same strain range the increase in the maximum width for the dent kernels varied from 476 to 680 μm, and for the flint kernels from 136 to 270 μm. In general the maximum width of the cracks occurred in the floury regions, the minimum occurring in the horny endosperm for all of the kernels tested. This was probably due to the fact that the floury endosperm fractures easily due to its weaker protein matrix and reduced bond area between the matrix and starch grains compared with the horny endosperm. Cracks which develop in the floury endosperm act as notches for the horny endosperm. Due to stress-concentration effects in the vicinity of the cracks, there is rapid crack propagation through the horny endosperm which in turn reduces the load-carrying capability of the kernels. Thus, the amount of floury region in a kernel should be minimized in order to maximize the kernel toughness.

In general, under most of the experimental conditions discussed, the flint kernels exhibited higher compressive properties than the dent kernels tested. It is believed that the flint kernels derived high strength due to the presence of higher proportions of the heavier protein matrix and their increased bond area between the matrix and the starch granules due to smaller and more-closely packed starch granules, compared with the floury endosperm.

It is likely that at very high compressive strain levels, which cannot be accommodated by crack initiation and extension, there will be deformation of individual starch granules and a change in the spacing between individual granules. At such high strains the properties of the kernels can be interpreted in terms of the theories of composite materials with spherical particles outlined in the Appendix.

## 6.3. Viscoelastic behaviour

The load–deformation data obtained from the stress relaxation tests were converted into a relaxation modulus–time relationship. The relaxation modulus curves at three levels of deformation velocity (1.27, 5.08 and 12.70 mm min$^{-1}$) for the kernels $H_2$ and $H_3$ are shown in Figs 13 and 14, respectively. Test data revealed that the magnitude of the relaxation modulus was not significantly influenced by deformation rate within the experimental range. Therefore, the data at each moisture level were merged and a generalized Maxwell model with three elements and a parallel spring was fitted to the available modulus data [11].

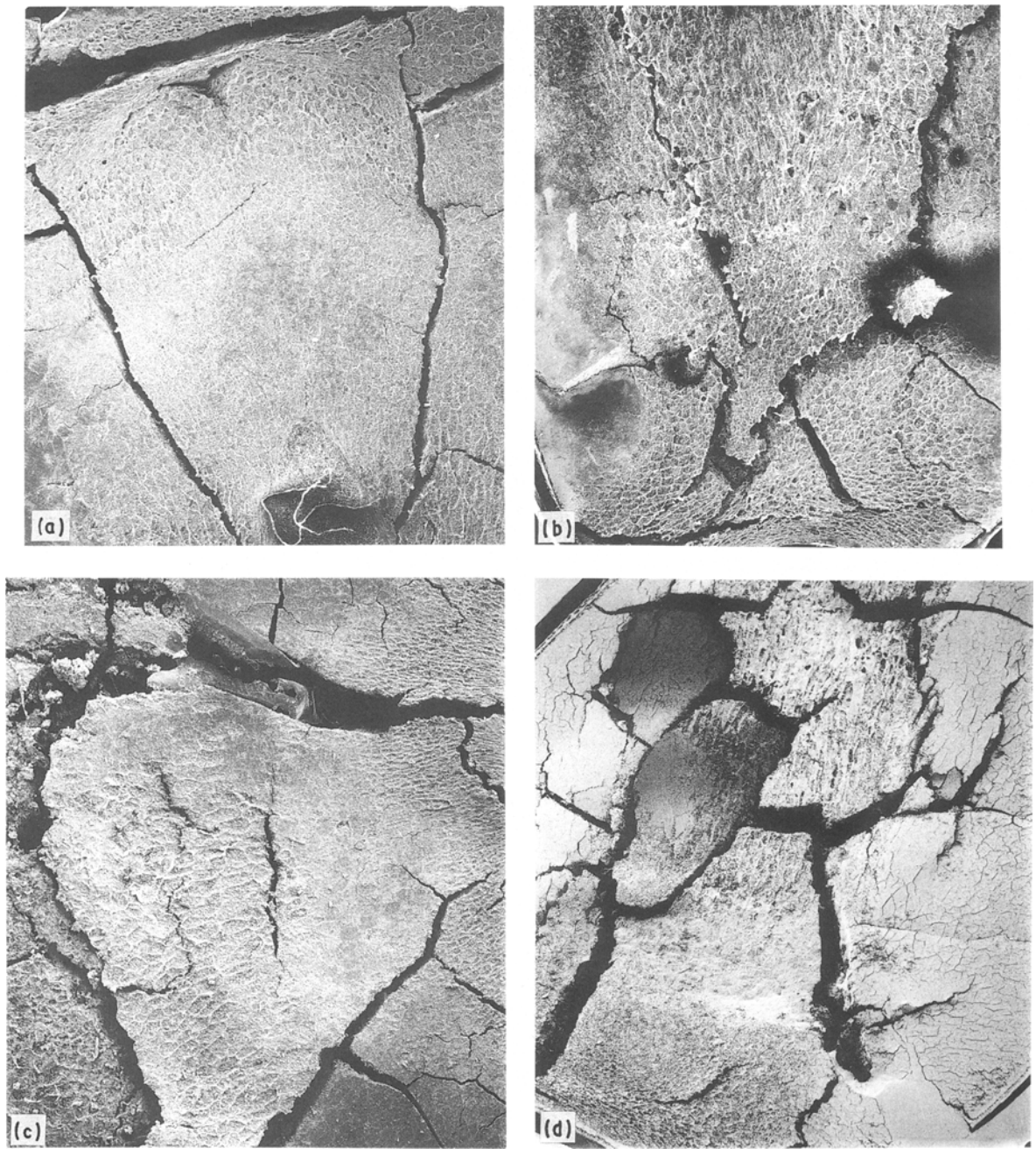


*Figure 10* Micrographs of the kernels subjected to compressive strains: (a) dent kernel at 15% strain (15 ×), (b) flint kernel at 15% strain (15 ×), (c) dent kernels at 25% strain (15 ×) and (d) flint kernels at 25% strain (15 ×).

TABLE I Maximum dimensions of the major primary cracks in the kernels as a function of strain

| Strain applied (%) | Corn species | Overall crack dimensions[a] | | | | Crack width in the horny endosperm (μm) |
|---|---|---|---|---|---|---|
| | | Length | | Width | | |
| | | *L* (mm) | *T* (mm) | *L* (μm) | *T* (μm) | |
| 0 | Dent | 0–2 | 0–4 | 0–68 | 0–68 | 0–8 |
| 0 | Flint | – | – | – | – | 0–3.5 |
| 15 | Dent | 0–5.27 | 0–4.08 | 0–102 | 0–476 | 0–1.2 |
| 15 | Flint | 0–5.44 | 0–3.74 | 0–102 | 0–136 | 0–1.5 |
| 25 | Dent | 0–6.29 | 0–4.93 | 0–493 | 0–680 | 0–12.8 |
| 25 | Flint | 0–6.12 | 0–3.97 | 0–374 | 0–270 | 0–10.2 |

[a] The maximum dimensions of the cracks appeared in the floury regions of the kernels. *L* represents the longitudinal crack dimensions and *T* represents the transverse crack dimensions.

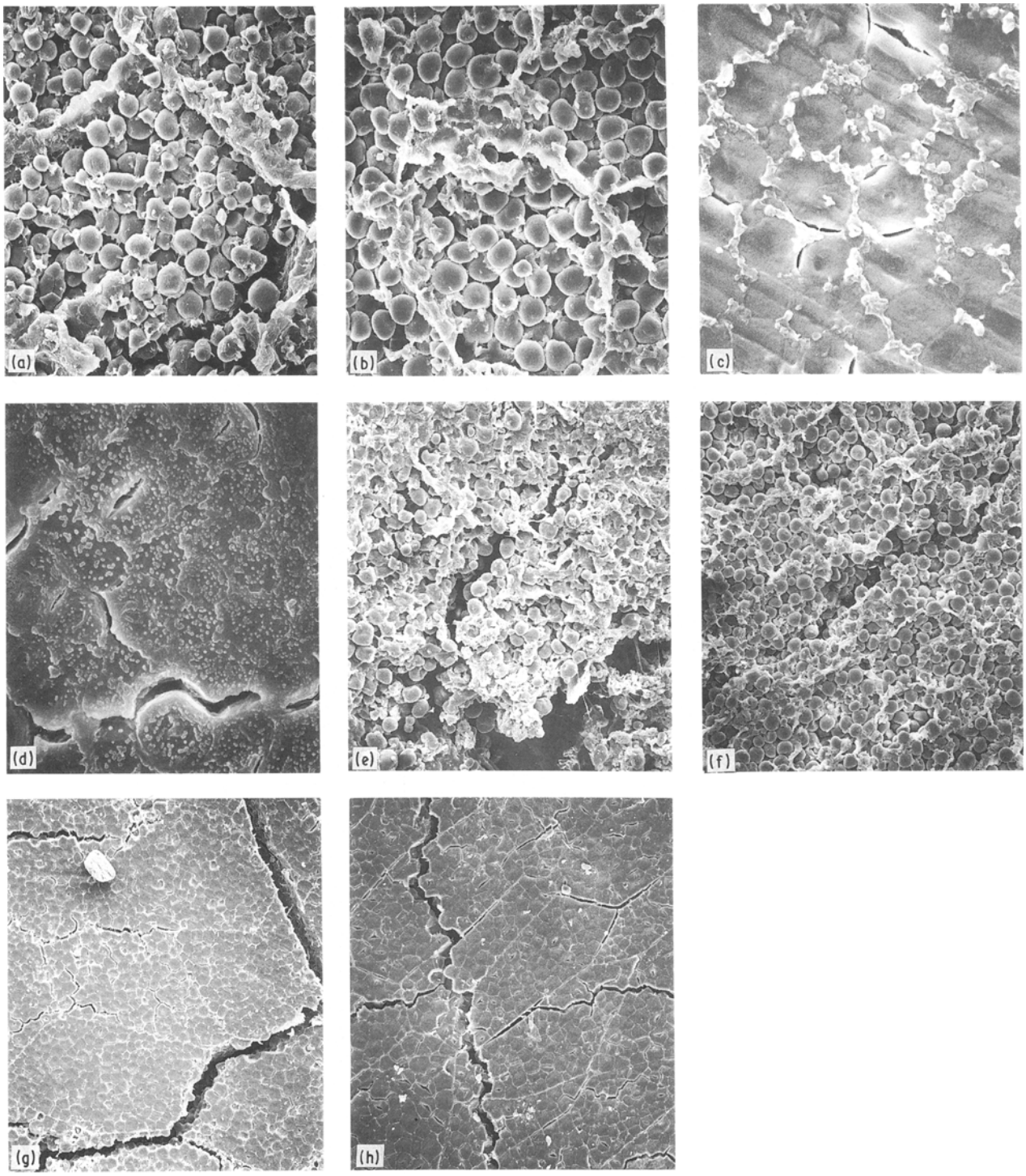


*Figure 11* Micrographs of the endosperms when the kernels were subjected to compressive strains: (a) dent floury endosperm at 15% strain (× 350), (b) flint floury endosperm at 15% strain (× 350), (c) dent horny endosperm at 15% strain (× 1200), (d) flint horny endosperm at 15% strain (× 1200), (e) dent floury endosperm at 25% strain (× 210), (f) flint floury endosperm at 25% strain (× 210), (g) dent horny endosperm at 25% strain (× 140) and (h) flint horny endosperm at 25% strain (× 140).

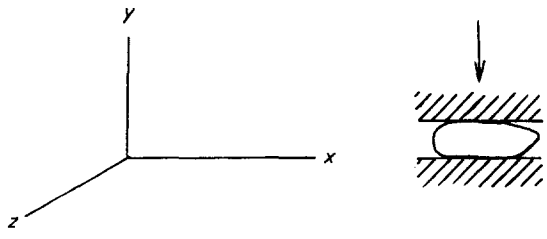


*Figure 12* Direction of compressive loads applied to the test kernels.

No definite trend could be established between the time of relaxation and the kernel moisture content, and the time of relaxation and the kernel type [11]. In most cases, at the beginning of relaxation the relaxation modulus values were considerably higher for the flint kernels ($H_3$) than for the dent kernels ($H_2$), especially in the moisture range 16 to 30%. However, as the time progressed, both of the kernels showed similar results.

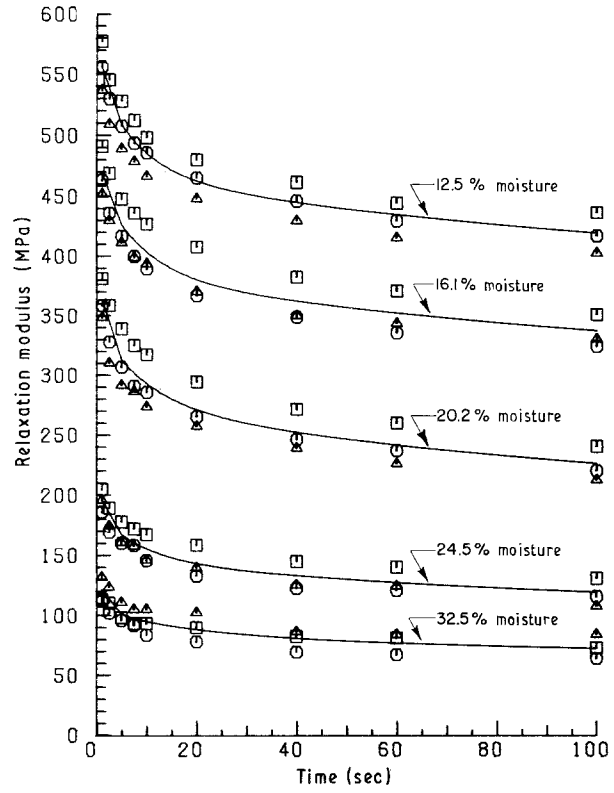


*Figure 13* Relaxation modulus of the dent kernels ($H_2$) as a function of time at five levels of kernel moisture content. Deformation velocity (□) 1.27, (○) 5.08 and (△) 12.70 mm min$^{-1}$.

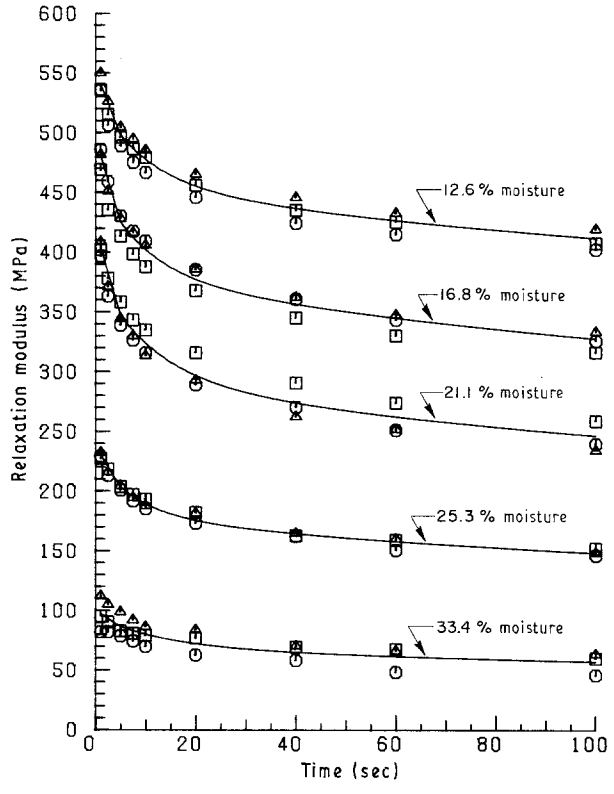


*Figure 14* Relaxation modulus of the flint kernels ($H_3$) as a function of time at five levels of kernel moisture content. Key as for Fig. 13.

In this paper, a best-fit model for a master relaxation modulus curve for the kernels of $H_2$ is presented. The functional relationship between the moisture shift factor and the kernel moisture content determined through regression analysis was

$$\ln a_M = 0.394 - 0.874(M - 20.2) \quad (r^2 = 99.1\%) \tag{13}$$

where $a_M$ is the moisture shift factor and $M$ is the moisture content (%).

Using this shift factor, a generalized Maxwell model of the form described in Equation 10 was fitted to the experimental data. The best-fit model consisted of six Maxwell elements and a parallel spring. The estimates of the model parameters are reported in Table II.

TABLE II Estimated parameters of the model for the master relaxation modulus function

| Maxwell element | Parameter | |
|---|---|---|
| | $E_i$ (MPa) | $\alpha_i$ (sec$^{-1}$) |
| 1 | 105.6 | 187.950 |
| 2 | 104.3 | 5.140 |
| 3 | 105.8 | 0.082 |
| 4 | 95.8 | 0.003 |
| 5 | 44.9 | 0.000 13 |
| 6 | 37.6 | 0.000 001 |
| Spring | 66.2 | – – – |

## 7. Conclusions

Based on the results obtained in this investigation, the following main conclusions were drawn.

1. Microscopic analysis revealed that the mechanical properties of corn kernels were influenced significantly by the kernel structures. The kernel strength levels were adversely affected by the presence of the floury endosperm in the kernels, as this endosperm cracks easily even at low loads or due to the drying stresses. These cracks in the floury endosperm behave like notches or flaws which lead to rapid crack propagation through the horny endosperm. As a result, the presence of floury endosperm causes a reduction in the kernel resistance to fracture. Therefore, proportions of the floury endosperms should be minimized by altering the genetic characteristic of the kernels in order to maximize the kernel toughness. A further increase in the toughness can also be achieved by developing the heavier protein matrix in the floury as well as in the horny endosperms.

2. The size of the longitudinal and transverse cracks in corn kernels increased with increasing strain or decreasing proportions of the horny endosperm.

3. The shape and size of the cells and the starch granules of the endosperms were not substantially altered by the strain within the range tested.

4. The ultimate stress, modulus of elasticity, and modulus of toughness were significantly higher for the flint kernels than for the dent kernels tested. This was primarily due to the higher proportions of horny endosperm with heavier protein matrix which is present in the flint kernels.

5. The modulus of resilience was not necessarily influenced by the kernel structure within the experimental range.

6. The ultimate stress, modulus of elasticity,

modulus of toughness and modulus of resilience decreased exponentially as the kernel moisture was increased. The values of ultimate stress, modulus of elasticity, modulus of toughness and modulus of resilience ranged from 8 to 82 MPa, 20 to 480 MPa, 0.8 to 4.4 MJ $m^{-3}$ and 0.2 to 0.8 MJ $m^{-3}$, respectively, in the moisture range 6 to 34% (wet basis).

7. The relaxation modulus of the corn kernels was influenced by the kernel structure only in the beginning of the relaxation process in the moisture range 16 to 34% (wet basis).

8. The relaxation modulus of the kernels was not significantly influenced by the deformation velocities in the range 1.27 to 12.7 mm $min^{-1}$.

9. The intact corn kernels were hydrorheologically simple materials over the range of moisture content considered. The master relaxation modulus curve can be adequately represented by a generalized Maxwell model with six elements and a parallel spring.

## Appendix: Theoretical model for the elastic properties of a particulate composite filled with dispersed reinforcement

Theoretical models are available to evaluate the elastic properties of a particulate composite at different levels of filler materials [29, 30]. A composite sphere model for a high volume fraction of the filler material described in this paper is suitable for the corn endosperms. The model is composed of a gradation of sizes of spherical particles in a continuous matrix. Each spherical filler particle of radius $a$ is assumed to be surrounded by a matrix layer of outer radius $b$. The ratio of $a/b$ is assumed to be constant for particles of any radius.

The model for shear modulus can be expressed as

$$\frac{G_c}{G_f} = \frac{1 - (1 - G_m/G_f)(7 - 5\mu_m + G_f/G_m)(1 - V_f)}{15(1 - \mu_m)} \quad \text{(A1)}$$

where $G$ is shear modulus, the indices c, m and f refer to the composite, matrix and filler, respectively, $\mu_m$ is the Poisson's ratio of the matrix and $V_f$ is the volume fraction of the dispersed filler.

The model for the bulk modulus is given by

$$\frac{K_c - K_m}{K_f - K_m} = \frac{V_f}{1 + [(1 - V_f)(K_f - K_m)/(K_m + \frac{4}{3}G_m)]} \quad \text{(A2)}$$

where $K$ is the bulk modulus.

The following expressions can be used to approximate the values of Young's modulus ($E_c$) and Poisson's ratio ($\mu_c$) of the composite materials for the computed values of shear modulus ($G_u$) and bulk modulus ($K_u$).

$$E_c = \frac{9K_cG_c}{3K_c + G_c} \quad \text{(A3)}$$

and

$$\mu_c = \frac{3K_c - 2G_c}{2(3K_c + G_c)} \quad \text{(A4)}$$

## References


1. J. BODIG and B. A. JANE, "Mechanics of Wood and Wood Composites" (Van Nostrand Reinhold, New York, 1982).
2. K. L. DORRINGTON, in "The Theory of Viscoelasticity in Biological Materials", Symposia of the Society for Experimental Biology, No. xxxiv (Cambridge University Press, London, 1980) p. 289.
3. Y. C. FUNG, in "Biomechanics: Its Foundations and Objectives", edited by Y. C. Fung, N. Perrone and M. Anliker (Prentice-Hall, Englewood Cliffs, New Jersey, 1972).
4. N. N. MOHSENIN, "Physical Properties of Plant and Animal Materials" (Gordon and Breach, New York, 1980).
5. N. N. MOHSENIN and C. T. MORROW, "Measurements of Viscoelastic Parameters in Food Materials. Rheology and Texture of Food Stuff", Science Monograph No. 27 (Society of Chemical Industries, London, 1968).
6. T. R. RUMSEY and R. B. FRIDLEY, *Trans. ASAE* (1977) 386, 392.
7. J. F. V. VINCENT, "Structural Biomaterials" (Macmillan, London, 1982).
8. K. G. SATYANARAYANA, K. K. RAVIKUMAR, K. SUKUMARAN, P. S. MUKHERJEE, S. G. PILLAI and A. G. KULKARNI, *J. Mater. Sci.* **21** (1986) 57.
9. L. A. BALASTREIRE, F. L. HERUM, K. K. STEVENS and J. L. BLAISDELL, *Trans. ASAE* **25** (1982) 1062.
10. L. SHELEF and N. N. MOHSENIN, *Cereal Chem.* **46** (1969) 212.
11. S. S. SINGH, PhD thesis, University of Wisconsin–Madison (1985).
12. G. C. ZOERB and C. W. HALL, *J. Agric. Res.* **5** (1960) 83.
13. K. G. SATYANARAYANA, A. G. KULKARNI and P. K. ROHATGI, *J. Sci. Indust. Res. (India)* **40** (1981) 222.
14. D. S. VARMA, M. VARMA and I. K. VARMA, *J. Reinforced Plast. Compos.* **4** (1958) 419.
15. L. G. GIBSON and M. F. ASHBY, "Cellular Solids – Structure and Properties" (Pergamon Press, New York, 1988).
16. S. S. SINGH, M. F. FINNER, P. K. ROHATGI and F. H. BUELOW, Inter-American Proceedings on Materials Technology, Vol. 1 (Southern Research Institute, San Antonio, Texas, 1989).
17. M. F. KUSTERMANN and H. D. KUTZBACH, ASAE Paper No. 82-3055, St Joseph, Michigan 49085 (1982).
18. L. A. BALASTREIRE, F. L. HERUM, K. L. STEVENSE and J. L. BLAISDELL, *Trans. ASAE* **25** (1982) 1057.
19. L. A. BALASTREIRE and F. L. HERUM, *ibid.* **24** (1978) 767.
20. J. R. HAMMERLE and N. N. MOHSENIN, *ibid.* **13** (1970) 372.
21. R. A. THOMPSON and G. H. FOSTER, Marketing Res. Rep. No. 631, USDA, Washington, DC (1963).
22. D. B. BROOKER, F. W. BAKKER-ARKEMA and C. W. HALL, "Drying Cereal Grains" (AVI Publishing, New York, 1978).
23. G. E. INGLETTE, "Corn: Culture, Processing, Products", edited by G. E. Inglette (AVI Publishing, New York, 1970) p. 123.
24. M. J. COX, M. M. MACMASTERS and G. E. HILBERT, *Cereal Chem.* **21** (1944) 447.
25. W. L. MASTERTON and E. J. SLOWINSKI, "Chemical Principles" (Saunders, Philadelphia, 1977).
26. J. D. FERRY, "Viscoelastic Properties of Polymers" (Wiley, New York, 1980).
27. R. M. CHRISTENSEN, "Theory of Viscoelasticity: An Introduction" (Academic Press, New York, 1971).
28. N. R. DRAPER and H. SMITH, "Applied Regression Analysis" (Wiley, New York, 1981).
29. R. M. CHRISTENSEN, "Mechanics of Composite Materials" (Wiley, New York, 1979).
30. A. A. BERLIN, S. A. VOLFSON, N. S. ENIKOLOPIAN and S. S. NEGMATOV, "Principles of Polymer Composites" (Springer-Verlag, New York, 1986).


*Received 18 August*
*and accepted 13 November 1989*